Runoff production on forest roads in a steep, mountain catchment

Beverley C. Wemple
Department of Geography, University of Vermont, Burlington, Vermont, USA

Julia A. Jones
Department of Geosciences, Oregon State University, Corvallis, Oregon, USA

Received 27 September 2002; revised 27 March 2003; accepted 21 May 2003; published 28 August 2003.

[1] This study investigated how roads interact with hillslope flow in a steep, forested landscape dominated by subsurface flow and how road interactions with hillslope flow paths influence hydrologic response during storms in a second-order catchment. Runoff was measured continuously from 12 subcatchments draining to road segments and covering 14% of a 101-ha, second-order catchment (WS3) in the Andrews Forest, Oregon. Observed runoff over the 1996 water year was compared to predictions for runoff timing and interception of a hillslope water table based on a simple model of kinematic subsurface storm flow. Observed runoff behavior was consistent with model estimates, a finding that underscores the utility of this simple approach for predicting and explaining runoff dynamics on forest roads constructed on steep hillslopes. Road segments in the study area interacted in at least four distinct ways with complex landforms, potentially producing very different effects depending on landform characteristics. Hillslope length, soil depth, and cutbank depth explained much of the variation in road runoff production among subcatchments and among storm events. Especially during large storm events, a majority of instrumented road segments intercepted subsurface flow and routed it to ditches and thence directly to streams with a timing that contributed to the rising limb of the catchment-wide hydrograph. The approach used in this study may be useful for model development and for targeting road segments for removal or restoration. *INDEX TERMS:* 1860 Hydrology: Runoff and streamflow; 1803 Hydrology: Anthropogenic effects; *KEYWORDS:* forest roads, subsurface flow, runoff production, hillslope hydrology

Citation: Wemple, B. C., and J. A. Jones, Runoff production on forest roads in a steep, mountain catchment, *Water Resour. Res.*, *39*(8), 1220, doi:10.1029/2002WR001744, 2003.

1. Introduction

[2] Roads are ubiquitous in steep, managed, forest lands, and they have been implicated in higher rates of water and sediment flux at the hillslope [*Megahan and Kidd*, 1972; *Reid and Dunne*, 1984] and catchment scale [*Janda et al.*, 1975; *Grant and Wolff*, 1991]. Roads may modify hydrology both through interception of precipitation on the road surface [*Luce and Cundy*, 1994; *Ziegler and Giambelluca*, 1997], and through interception of subsurface flow [*Megahan*, 1972; *Megahan and Clayton*, 1983]. Hydrologic modifications imposed by roads have also been implicated in geomorphic effects, including increased channelization of hillslopes [*Montgomery*, 1994; *Croke and Mockler*, 2001] and mass wasting [*Anderson*, 1983; *Wemple et al.*, 2001].

[3] This study addresses two key unresolved issues in road hydrology [*Luce*, 2002]: the mechanisms by which forest roads intercept and route water, and how this understanding can be used to guide road restoration efforts. We focus on the interaction of subsurface flow with roads, which is an important process in forest lands. Surface area occupied by roads is often small relative to the hillslope areas intercepted by road cuts on steep slopes. The interaction between subsurface flow pathways and the road is a critical aspect of forest road hydrologic behavior. In general, soil properties and hillslope topography control flow pathways in forested landscapes [*Dunne et al.*, 1975; *Anderson and Burt*, 1978; *O'Loughlin*, 1981; *Montgomery and Dietrich*, 1995; *Woods and Rowe*, 1996; *McDonnell et al.*, 1996]. Hydraulic conductivity of highly permeable forest soils typically declines with depth, leading to the development of perched, sometimes discontinuous saturated zones during storms [*Harr*, 1977] that may be intercepted by roads. Subsurface flow intercepted along the road cut may be diverted to surface runoff [*Megahan*, 1972], modifying preexisting flow paths in the catchment. Identifying these sites may aid in prioritizing road segments for restoration or decommissioning.

[4] The hydrologic behavior of a road network in a catchment depends upon the behavior of individual road segments, which can be demarcated by drainage divides along the road. Each segment of a forest road acts as a subcatchment collecting some portion of the surface and subsurface flow from above the road (Figure 1). For each road segment, the relevant subcatchment consists of the hillslope above the road, the road surface, and the roadside ditch draining to the culvert. In steep terrain, roads are typically constructed parallel to hillslope contours using cut and fill road designs, in which roughly half of the road

0043-1397/03/2002WR001744

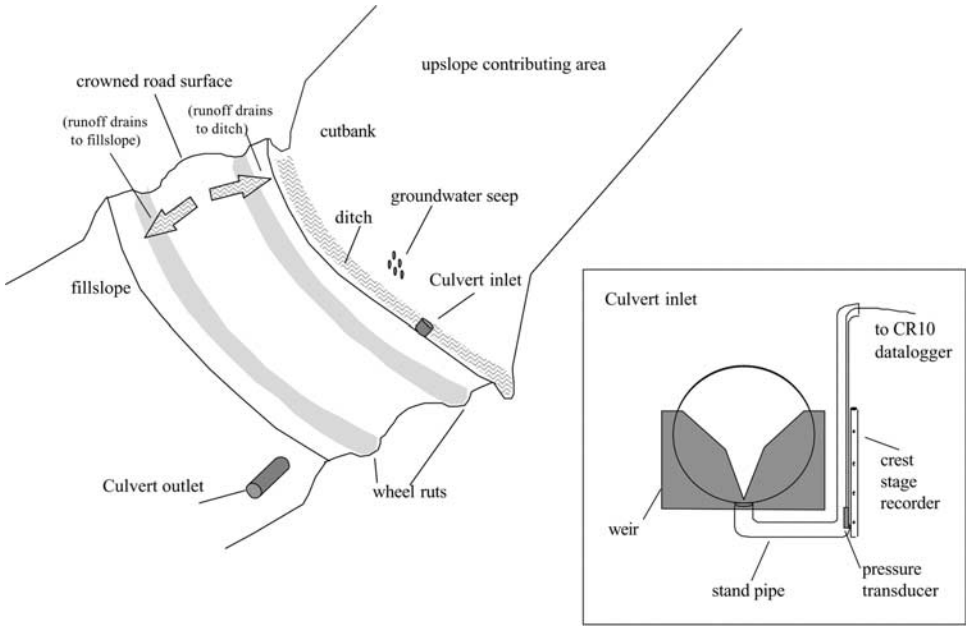

Figure 1. Schematic representation of cut-and-fill forest road, showing drainage area contributing to a road segment. Inset illustrates gaging system installed at culvert inlets for this study.

surface is cut into the slope (the road cut), and half is perched on fill material (the fill slope) [*Pearce*, 1961]. Upslope of the road is a cut bank of varying depth and an inboard ditch. The ditch captures flow draining through or over the hillslope above the cut slope, as well as runoff from the road surface, and routes this flow to a culvert. Downslope of the road is an oversteepened area of fill supporting the outside of the road. Roads may be either insloped (draining runoff to the ditch), outsloped (draining runoff to the fill slope), or crowned (flow drains to both ditch and fill slope).

[5] The properties of the subcatchment draining to a road segment should be related to runoff from the road segment. The amount of overland flow produced on the road should be related to the permeability and area of road surface contributing to the ditch [*Luce and Cundy*, 1994; *Ziegler and Giambelluca*, 1997]. The amount of subsurface flow interception should be related to the hillslope area above the road and interaction of the road cut with subsurface flow paths [*Megahan*, 1972; *Megahan and Clayton*, 1983].

[6] The collective contribution of a road network to the hydrologic response of a catchment depends upon how the road segments in the catchment modify the capture and routing of flow to the stream channel. In the pre-road condition, the storm hydrograph in a catchment comprises the contributions from a set of hillslope segments draining to channels. Roads constructed parallel to contour in mid-slope positions create new subcatchments with shorter hillslope lengths, and the runoff they capture may be routed directly to a stream channel [*Wemple et al.*, 1996]. If roads intercept large amounts of subsurface flow and route it directly to channels, they might alter peak discharge magnitude and change catchment-scale response time [*King and Tennyson*, 1984; *Jones and Grant*, 1996]. This proposition has been controversial [*Thomas and Megahan*, 1998; *Beschta et al.*, 2000; *Jones and Grant*, 2001; *Thomas and Megahan*, 2001]. Recent modeling studies suggest that the ability of individual road segments to intercept subsurface flow, and the arrangement of these segments relative to the stream channel network, determine road network effects on catchment-scale response [*Bowling and Lettenmeier*, 2001; *Tague and Band*, 2001]. Road segments whose storm hydrographs contribute to the rising limb of the catchment-scale hydrograph are most likely to contribute to speeding the overall hydrologic response of a catchment, and therefore might be targeted for restoration.

[7] In this study, we addressed two questions related to runoff production on roads and the potential effect on catchment-scale hydrologic response in a steep, forested catchment: (1) Can the relative magnitude and timing of road runoff be predicted from mappable characteristics of the subcatchment draining to a road segment? (2) Do road segments produce storm hydrographs whose magnitude and timing might contribute to augmenting and speeding hydrologic response in a small catchment?

2. Methods

2.1. Approach

[8] A series of steps were involved in answering these questions. The contributing areas for each road segment were mapped. Runoff and precipitation were measured along a series of road segments over part of the 1996 water year. Runoff from each road segment was predicted using a simple linear rainfall-runoff relation to estimate contributions from road surfaces and a kinematic approximation of subsurface flow to estimate interception along road cuts. Observed and predicted runoff patterns were compared among the monitored road segments, and between road segments and the catchment scale.

2.2. Study Site

[9] Watershed 3 (WS3) is a 101-ha catchment in the Lookout Creek watershed in the western Oregon Cascades (Figure 2). Streamflow, sediment yield, vegetation cover, and other environmental variables have been monitored in WS3 since 1952 as part of a paired-catchment experiment at

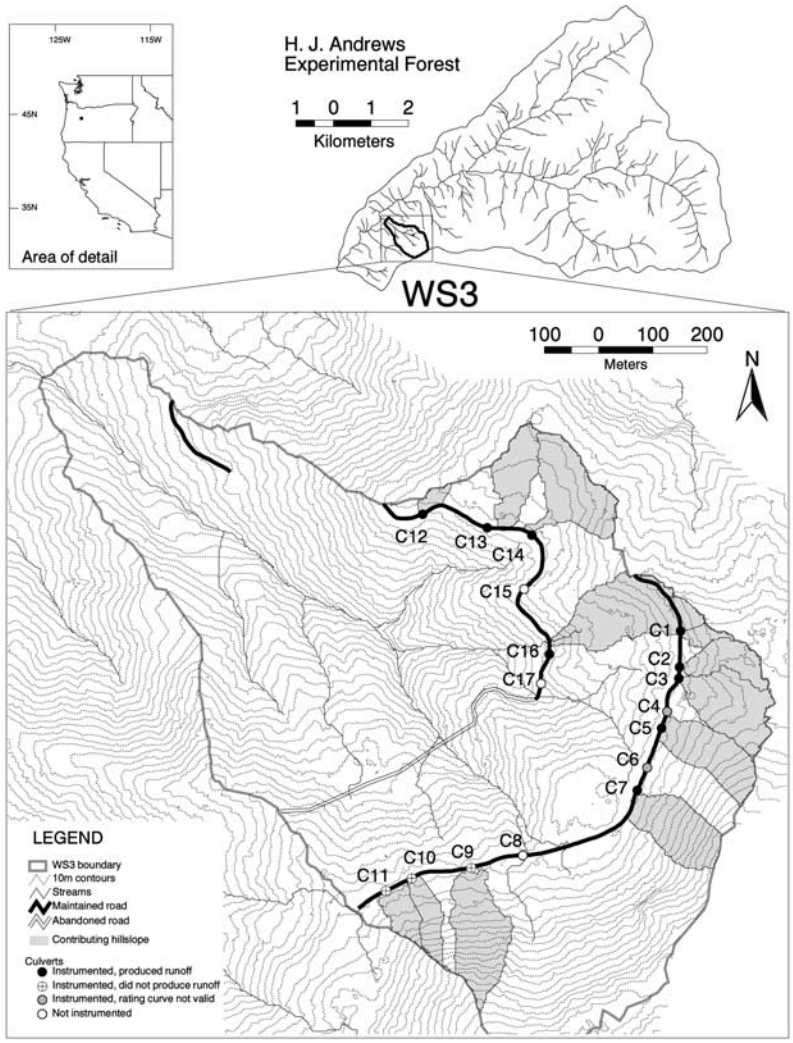

Figure 2. Study area, watershed 3 (WS3) at the H. J. Andrews Experimental Forest. Location of roads, culverts, and instrumentation are shown.

the H. J. Andrews Experimental Forest [*Rothacher et al.*, 1967; *Jones and Grant*, 1996; *Jones*, 2000]. Elevation ranges from 480 to 1080 m. The catchment-wide average hillslope gradient is 53%, and stream channels originate from source areas of 1 to 3 hectares [*Wemple et al.*, 1996]. Mean annual precipitation is 2300 mm, with approximately 80% occurring between October and April [*Greenland*, 1994]. Precipitation occurs most frequently in the form of rain at this elevation, but almost half of the peak runoff events are ''rain-on-snow'' events, in which rain falls on an accumulated snowpack [*Harr*, 1981; *Perkins*, 1997].

[10] The catchment is underlain by rocks of volcanic origin, including andesite lava flows and breccias [*Swanson and James*, 1975]. The oldest rocks, generally occurring at elevations below 900 m, are of late Oligocene to early Miocene age and consist of massive blocky breccias and welded and nonwelded ash flows. Capping the older volcaniclastic rocks is a younger, more stable rock formation of andesite flow rocks of middle to late Miocene age. Both deep-seated and shallow mass movements occur on volcaniclastic substrates, especially in the contact zone where flow rock caps clastics. Inactive deep-seated slumps form prominent benches and irregular hillslope profiles, particularly on the upper hillslopes in the catchment. In many locations bowl-shaped depressions, indicating shallow translational slides, are superimposed on these profiles. Exposures along road cuts in WS3 suggest that these depressions are mantled with colluvium derived from the ridge-capping andesite rock. Soil depths range from less than a meter along ridges to more than 4 m along the axis of topographic depressions. Soils are generally underlain by saprolite of relatively low conductivity or in some locations by deep deposits of unconsolidated colluvium [*Rothacher et al.*, 1967]. In this environment, soil permeability decreases with depth, often leading to the development of discontinuous saturated zones at the soil-subsoil interface and preferential subsurface flow during storms [*Harr*, 1977]. Vegetation cover is forest, dominated by old-growth Douglas fir (*Pseudotsuga menziesii*), western hemlock (*Tsuga heterophylla*) and western red cedar (*Thuja plicata*) [*Rothacher et al.*, 1967]. In 1963, roughly 25% of the forest cover was clearcut in three 8-ha patch cuts that were broadcast burned and replanted with Douglas fir.

[11] In 1959, 2.7 km of logging road were constructed in three tiers (lower, middle and upper roads), parallel to hillslope contours (Figure 2). At an average width of 5 m,

Table 1. Characteristics of 12 Road Segments Instrumented to Measure Continuous Runoff During 1996 Water Year in Watershed 3, Andrews Forest, Western Oregon

Segment	Contributing Area: Road Surface A_r, m^2	Contributing Area: Hillslope A_h, ha	Slope Length X, m	Slope Gradient α, %	Soil Depth D_s,[a] m	Cutbank Depth D_{rc}, m	Period of Record[b]	Number of Precipitation Events[c]	Number (Percent) of Peak Runoff Events[c]	Road Surface as Percent of Total Runoff[d]
C1	32	0.16	65	64	0.75	8.4	full	30	18 (60)	3.7
C2	42	0.78	150	40	1.5	3.1	full	30	18 (60)	0.9
C3	123	1.64	230	38	2.0	2.9	full	30	16 (53)	1.1
C5	50	1.32	240	58	>4.0	1.7	early	19	6 (32)	0.9
C7	20	1.49	275	72	>4.0	5.4	full	30	18 (60)	0.3
C9	5	1.89	400	72	>4.0	0	early	19	0 (0)	na
C10	5	0.59	225	64	0.25	2.5	early	19	0 (0)	na
C11	7	0.55	150	57	0.25	1.5	early	19	0 (0)	na
C12	100	0.16	100	45	1.0	4.5	middle	8	5 (63)	6.7
C13	12	1.07	120	26	> 4.0	0	early	14	9 (64)	1.3
C14	30	1.75	150	42	> 4.0	0.3	full	30	15 (50)	0.5
C16	35	2.54	150	57	0.5	2.0	early	19	16 (84)	0.4

[a]Soil depth immediately above the road cut as determined by drive probe measurements (see text). Depths measured to the nearest 0.25 m. Depths exceeding maximum measurement depth of 4.0 m are indicated.

[b]Early season is November 1995 to 7 February 1996; middle season is 15 January to 15 March; full season is November 1995 to April 1996. Record unavailable due to instrument malfunction at the following sites/dates: (1) at all sites during storms of 21 March and 30 March, (2) at C1, C2, C3, C5, C7 during storm of 27 November, (3) at C13 between 16 December and 16 January, (4) at C14 and C16 during storm of 14 January, and (5) at C9, C10, C11 during storm of 4 February.

[c]Number of precipitation events and number of peak runoff events (as defined by algorithms described in text) measured at each site during the monitoring period. Number of precipitation events is taken from Table 2 minus events during which records are missing for culverts (see footnote b). Number of peak runoff events is followed by percentage of precipitation events that produced a peak runoff response.

[d]Values are derived from calculated estimates of runoff from road surfaces for all precipitation events (listed as number of precipitation events in table) during the monitoring period for each site using equation (1), divided by total cumulative runoff measured at each site.

the compacted road surface and ditch of the WS3 road network occupies approximately 1.3% of the catchment area. The roads are of cut-and-fill design, consisting of a cutbank, an inboard ditch, a crowned road surface, and a fill slope (Figure 1). Each ditch collects runoff from a road segment of 5 to 100 m in length and routes it to one of two culvert types: ditch relief culverts, which transmit accumulated ditch flow to hillslopes below roads, and stream-crossing culverts, which provide crossings for stream channels. Ditch flow along a given road segment may be collected from overland flow generated on the road surface or from subsurface flow intercepted along the cut slope. A debris slide in 1971 resulted in closure of a portion of the middle road in WS3 (Figure 2). No vehicle traffic occurred on the roads during the study period.

2.3. Delineation and Mapping of Subcatchments Draining to Roads

[12] The subcatchment draining to each culvert, defined as the contributing road surface and hillslope above the road segment (Figure 1), was mapped and measured using a combination of field and GIS measurements. Subcatchments were denoted with a C followed by a number: C1, C2, etc. Boundaries for contributing road surfaces were delimited by natural drainage divides between adjacent culverts following *Wemple et al.* [1996]. Maps of the actual road surface areas contributing runoff to each culvert were constructed during storm events in November and December of 1995 by introducing dye to road surface flow, observing flow paths, and mapping the area in a manner similar to that developed by *Reid* [1981].

[13] The contributing hillslope for each site was determined based on surface topography using a digital elevation model with a 3 m grid cell resolution generated from remotely sensed lidar data. The cell along the road segment with the maximum contributing area was designated as the outlet for the hillslope. Convergent hillslopes with contributing areas greater than 0.5 ha (see Table 1) produced clearly distinguishable subcatchments that could be associated with ten of the twelve road segments on the digital elevation model (Figure 2). Drainage areas at C1 and C12 were determined by manually digitizing the hillslope bounded by the road surface draining to the culvert. Bedrock topography may route subsurface water somewhat differently than implied by surface topography [*McDonnell et al.*, 1996], and the road cutbank may intercept flow paths not included in the surface-topography-based contributing area. Therefore the actual area draining to the road segment may also include some of the triangular interfluves between adjacent mapped contributing areas.

[14] The cutbank depth, soil depth, and soil type were determined for each instrumented road segment. Cutbank depth was measured along the road cut at 25-m intervals by recording level readings on a stadia rod held in the ditch. Soil unit descriptions and estimates of soil depth were taken from *Dyrness* [1969]. We supplemented these with measurements of soil depth to a maximum of 4 m at approximately 50-m intervals immediately upslope of the road using a hammer to drive a galvanized steel pipe into the soil profile [*Wemple*, 1998].

2.4. Flow Instrumentation and Runoff Estimation

[15] Twelve culverts draining subcatchments whose collective area amounted to 16% of the 101-ha WS3 were instrumented from November 1995 through April 1996 to determine runoff produced on roads (Figure 2 and Tables 1 and 2). A single weir at each culvert collected runoff generated from the road surface and the cut slope (Figure 1).

Table 2. Summary of Precipitation Events During the Study Period November 1995 to April 1996

	Storm Date, Time[a]	Precipitation Depth,[b] mm	Average Intensity,[b] mm/hr	Maximum Intensity,[b] mm/hr	Duration,[2] hours	Minimum/ Maximum Temperature,[b,c] °C	Form[d]
1	24 Nov., 0030*	103	1.5	7.1	69.0	2.8/9.4	r
2	27 Nov., 0630*	55	1.6	7.1	34.0	7.8/10.1	r
3	29 Nov., 0900*	51	2.5	6.1	20.0	7.3/9.5	r
4	30 Nov., 1100*	41	1.7	4.6	23.5	2.5/9.3	r
5	1 Dec., 1800	23	0.7	3.3	25.5	1.5/4.0	r
6	3 Dec., 1200	20	1.1	4.2	20.5	1.3/7.3	r
7	5 Dec., 0330	24	1.7	7.6	20.5	0.5/2.6	r
8	8 Dec., 0300*	44	1.6	6.6	32.5	0.9/9.1	r
9	10 Dec., 1200	82	1.3	6.6	79.0	2.5/8.4	r
10	14 Dec., 0600	25	1.3	6.6	15.0	1.3/4.9	r
11	28 Dec., 1200*	165	2.6	9.1	70.0	2.8/10.2	r
12	2 Jan., 2030	25	1.3	3.3	20.0	5.4/9.7	r
13	4 Jan., 0030	29	0.8	3.0	48.0	1.4/3.7	r
14	7 Jan., 0500*	45	2.1	5.1	24.0	5.2/6.7	r
15	9 Jan., 0100	28	1.5	4.0	19.5	2.9/6.2	r
16	14 Jan., 1200*	79	1.4	8.6	73.5	−0.6/7.2	m
17	18 Jan., 0830*	172	1.9	7.6	81.0	−0.7/1.3	m
18	22 Jan., 1700	98	1.2	5.1	91.0	−1.5/0.2	s
19	26 Jan., 2000	75	1.3	6.1	72.0	−1.9/0.3	s
20	4 Feb., 2200	259	4.5	12.2	68.0	1.8/8.1	m
21	8 Feb., 0030	47	2.1	10.5	27.5	5.8/8.8	m
22	17 Feb., 1500	55	1.8	3.5	35.0	1.6/8.5	m
23	20 Feb, 0030	73	1.3	6.1	102.0	−2.3/8.1	m
24	3 March, 0230	34	1.0	4.1	52.5	0.6/5.2	m
25	10 March, 1200	9	1.2	5.1	12.0	7.6/9.5	r
26	11 March, 0630	9	0.7	1.8	21.0	4.5/8.9	r
27	21 March, 1900	14	0.8	3.7	28.0	-	-
28	30 March, 2100	69	1.4	4.0	61.0	-	-
29	9 April, 1400	59	1.0	4.0	82.0	0.6/9.2	m
30	15 April, 1700	23	1.1	3.6	32.0	0.8/13.3	r
31	17 April, 0930	23	1.1	11.7	36.5	1.0/5.1	r
32	19 April, 0630	19	0.8	3.2	35.0	0.5/5.6	r
33	21 April, 0800	114	1.6	9.7	83.5	2.2/9.5	r

[a]Storm date, time indicate start of precipitation event. Asterisks indicate nine storms prior to February 1996 used for cross-site analysis (10 December event is eliminated from cross-site analysis due to suspected data errors).
[b]Storm statistics, including total precipitation depth, average precipitation intensity, maximum one-half hour precipitation intensity, and maximum/minimum temperatures are given for the storm period, defined by the begin time and end time of precipitation.
[c]Minimum and maximum temperatures recorded on CR10 datalogger at the 466 road. Dashes indicate data not available.
[d]Precipitation form, classified as rain (r), mixed rain and snow or rain-on-snow (m), or snow (s), see text.

Five of the 17 culverts in WS3 were not instrumented: two ditch-relief culverts (C8 and C15) were blocked by sediment, and a stream-crossing culvert (C17) could not be gaged using the technology available. Two additional ditch-relief culverts (C4 and C6) were initially instrumented but abandoned, due to difficulty in rating the 9-inch (23 cm) pipes that were frequently submerged during storms.

[16] All 12 instrumented culverts were ditch-relief culverts constructed of 18-inch (46 cm) corrugated metal pipe. An aluminum plate V-notch weir with a double 60° to 120° notch was attached to each culvert inlet. Stage at the weir was measured by 2.5-psi pressure transducers (Electronic Engineering Innovations, Las Cruces, NM) installed in stand pipes constructed of 6 cm diameter polyvinyl chloride (PVC) pipe. Transducer output (in millivolts) was converted to water height above datum using calibration equations established in laboratory measurements over temperature ranges of 2° to 15°C. Stage readings were recorded at 5-minute intervals using CR10 data loggers (Campbell Scientific, Logan, UT). Peak stages at each installation were verified weekly using manual crest-stage recorders of 2.5 cm diameter PVC pipe with a dip stick and floating cork. Discharge was calculated from a common rating curve based on 24 measurements of stage height (ranging from 1.8 to 19 cm) with corresponding discharge (ranging from 30 to 23,000 mL/s) determined from volumetric measurements of flow over timed intervals [*Wemple*, 1998].

[17] Air temperature was measured at 15-minute intervals at each CR10 data logger using a shielded thermocouple. Precipitation data at 15-minute intervals were obtained from the tipping bucket rain gage at the Primet meteorological station at the Andrews Experimental Forest headquarters, located 1.4 km from the gaging station at WS3.

[18] Runoff monitoring on WS3 roads began in November 1995 at all instrumented sites, except C12, where monitoring began on 16 January 1996 (Table 1). On 6 February 1996, a debris flow during the flood of record destroyed the gage at WS3 and the installations at C5, C13, and C16. Damage to data loggers during the flood event destroyed data files at C9, C10 and C11 (Table 1). Continuous data for all sites (except C12 beginning on 16 January 1996) were available for comparison to WS3 between 16 November 1995 and 4 February 1996. Monitoring continued at five sites (C1, C2, C3, C7, C14) until April 1996.

[19] Precipitation events and peak runoff events were selected from continuous records of precipitation and runoff

Table 3. Model Parameters, Sources, and Values or Ranges Used in Calculations

Parameter	Symbol	Value/Range	Source/Comments
Hydraulic conductivity parameter (m/hr)	K_o	2.21	*Harr* [1977] as discussed by *Beven* [1982a]
Hydraulic conductivity parameter	n	1.2	*Harr* [1977] as discussed by *Beven* [1982a]
Moisture content parameter	θ_o	0.613	*Harr* [1977] as discussed by *Beven* [1982a]
Moisture content parameter	m	0.037	*Harr* [1977] as discussed by *Beven* [1982a]
Soil tension at air entry (kPa)	ψb	1	*Clapp and Hornberger* [1978] as discussed by *Beven* [1982a]
Soil moisture parameter	B	5	*Clapp and Hornberger* [1978] as discussed by *Beven* [1982a]
Initial soil moisture tension (kPa)	ψo	20–100	range taken from *Beven* [1982a]
Input rate (m/hr)	i	see Table 2	values reflect range of average precipitation rates, r and adjusted per equation (11)
Slope length above road cut (m)	L	see Table 1	values taken from measured slope lengths, X and adjusted per equation (12)
Slope gradient above road cut (radians)	α	see Table 1	values used to reflect range of measured slope angles (in degrees) and converted to radians
Soil depth at road cut (m)	D	see Table 1	values taken from measured soil depths, D_s and adjusted per equation (13)
Depth of road cut (m)	D_{rc}	see Table 1	values taken from measured road cut depths

using two automated procedures. Precipitation events were defined as periods of at least 12 hours with average precipitation intensity exceeding 0.5 mm/hour, following a >6 hour period without precipitation. Precipitation events were classified following *Perkins* [1997] as rain if air temperature exceeded 1°C throughout the event; as "mixed" if the minimum temperature was less than 1°C and the maximum temperature was above 1°C, and as snow if the maximum temperature was below 1°C. Peak runoff hydrographs from road segments were defined as periods beginning with an increase of >1.5 cm in stage height and ending either when stage height fell to 20% of the peak height or after a 72 hour period with steadily declining flow. Peak runoff hydrographs for WS3 were selected from the continuous streamflow record www.fsl.orst.edu/lter) based on the criteria outlined by *Jones and Grant* [1996].

[20] Precipitation and runoff events were matched if the rise in runoff began within 24 hours of the start of precipitation. Although 33 precipitation events were recorded at the Primet meteorological station during the monitoring period (Table 2), instrument malfunction or flood damage resulted in a variable number of precipitation events monitored at each site, ranging from a minimum of 8 to a maximum of 30 events (Table 1). Among these precipitation events, a variable number of runoff events, ranging from 0 to 18, were detected at each site. A subset of nine storms between 24 November and 4 February that produced runoff at multiple sites and at WS3 were used for cross-site analysis (Table 2). Damage to instrumented sites and destruction of the WS3 gage during the 4–8 February 1996 flood prevented meaningful cross-site comparisons after this period.

2.5. Estimation of Road Surface Runoff

[21] Infiltration rates on forest roads are typically one or more orders of magnitude lower than surrounding native soils [*Reid*, 1981; *Luce and Cundy*, 1994; *Ziegler and Giambelluca*, 1997]. We generated liberal estimates of surface runoff on each road segment, assuming no infiltration into the road bed. Surface runoff (q_r) for each road segment was estimated from precipitation records with a linear rainfall-runoff relation of the form

$$q_r = \sum_{j=1}^{n} c p_j A_r \tag{1}$$

where c is a runoff coefficient, set equal to unity for all storms, A_r is the road surface area draining to the instrumented culvert, and p_j is the total precipitation depth for event j during which road segment instrumentation was functional, permitting monitoring of total runoff from the road segment drainage area. The total number of storms for which equation (1) was applied varied across sites, according to the availability of runoff records from the monitored road segment. To estimate the fraction of road surface runoff produced on each road segment, we divided the results of (1) by the by the total cumulative runoff measured at each site over the monitoring period (Table 1).

2.6. Predictions of Subsurface Flow Interception on Roads

[22] Theoretical predictions of hillslope water table elevation and timing of runoff response were generated using the analytical solutions of *Beven* [1982a, 1982b] for kinematic subsurface storm flow on inclined slopes and compared to observations of runoff behavior from road segments. These solutions presume that hillslope seepage occurs in response to formation of a saturated zone on the hillslope following precipitation. Observations of subsurface flow dynamics at other sites near our study area confirm that discontinuous saturated zones develop on these steep hillslopes during storm events [*Harr*, 1977]. Subsequent study in WS3 has shown that perched saturated zones develop and contribute to seeps along road cuts [*Dutton*, 2000; B. Wemple, unpublished data].

[23] Predictions were made under assumptions of constant precipitation inputs over a range of conditions consistent with site and storm characteristics for our study area and study period. Soil conditions were assumed to vary with depth through the profile in a manner consistent with field observations at a nearby catchment [*Harr*, 1977]. Saturated hydraulic conductivity, K(h), and moisture content, θ(h), were expressed as

$$K(h) = K_o h^n \tag{2}$$

$$\theta(h) = \theta_o h^m \tag{3}$$

where parameters K_o, n, θ_o and m describe the form of hydraulic conductivity and porosity variation with depth through the soil profile and can be derived from field data (Table 3).

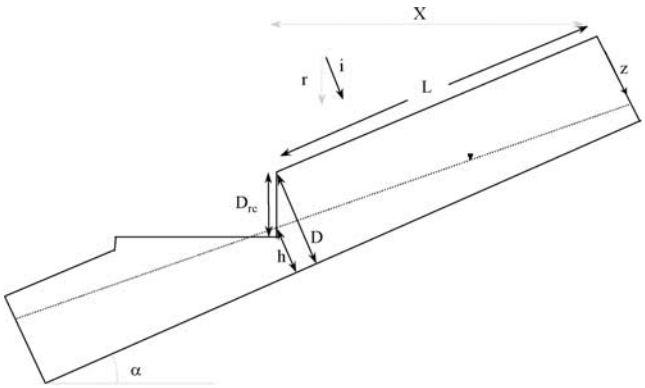

Figure 3. Schematic diagram illustrating the interaction of the hillslope water table with the road cut and parameters used in calculations.

[24] Two components of hillslope timing were estimated, using Beven's approach for response time of the unsaturated zone and saturated zone. The unsaturated zone response time (Tuz) reflects the lag between start of rainfall and start of runoff and is sensitive to variation in rainfall rate, initial soil moisture conditions and soil depth. The unsaturated zone response time was expressed as

$$\mathrm{Tuz} = 1/\mathrm{i}\Big[(\mathrm{a}/1+\mathrm{b})\left(\mathrm{D}^{1+\mathrm{b}} - \mathrm{h}_\mathrm{w}^{1+\mathrm{b}}\right) - (\theta_o/1+\mathrm{m})\left(\mathrm{D}^{1+\mathrm{m}}(\psi_\mathrm{b}/\psi_\mathrm{o})^{1/\mathrm{B}} - \mathrm{h}_\mathrm{w}^{1+\mathrm{m}}\right)\Big] \quad (4)$$

where i is a constant input rate to the hillslope, ψ_b is capillary tension at air entry, ψ_o is initial soil moisture tension, B is a parameter that reflects the pore size distribution of the soil, and $h_w = (i/K_o \cos \alpha)^{1/n}$. The parameter D is soil depth measured orthogonal to the slope and α is the gradient of the hillslope (Figure 3). Constants a and b relate soil water content to elevation of the water table as given by *Beven* [1982a, 1982b]

$$\mathrm{a} = \theta_o(\mathrm{i}/\mathrm{K_o}\cos\alpha)^{1/(2\mathrm{B}+3)} \quad (5)$$

$$\mathrm{b} = \mathrm{m} - (\mathrm{n}/2\mathrm{B}+3) \quad (6)$$

The saturated zone response time (Tc) reflects the delay between start of runoff and time at which the hillslope reaches steady state conditions, and is sensitive to variation in rainfall rate, slope length and slope gradient. The time to concentration was expressed as

$$\mathrm{Tc} = 1/\mathrm{i}\left[(\theta_\mathrm{o}/1+\mathrm{m})\left(\mathrm{h}_\mathrm{L}^{1+\mathrm{m}} - \mathrm{h}_\mathrm{w}^{1+\mathrm{m}}\right) - (\mathrm{a}/1+\mathrm{b})\left(\mathrm{h}_\mathrm{L}^{1+\mathrm{b}} - \mathrm{h}_\mathrm{w}^{1+\mathrm{b}}\right)\right] \quad (7)$$

where $h_L = [(n + 1)\ i\ L/K_o \sin \alpha]^{1/(1+n)}$, L is length of the hillslope (Figure 3), and other variables are as defined above. The time to steady state or equilibrium conditions (Te) for the hillslope is the sum of the unsaturated and saturated zone response times, e.g.,

$$\mathrm{Te} = \mathrm{Tuz} + \mathrm{Tc} \quad (8)$$

When precipitation ceases before the time to equilibrium, transient conditions prevail, and the hydrograph will peak when a drying front on the hillslope reaches the water table sometime after Tuz but before Te in a manner described by *Beven* [1982b].

[25] The elevation of the steady state water table at the cutbank of each instrumented road segment was estimated as:

$$\mathrm{h} = [(\mathrm{n}+1)\ \mathrm{i}\ \mathrm{L}/\mathrm{K_o}\sin\alpha]^{1/(1+\mathrm{n})} \quad (9)$$

where L is slope length from the ridge to the cutbank above the road (Figure 3). The elevation of the water table relative to the base of the road cut (h_{rc}) was calculated as:

$$\mathrm{h_{rc}} = \mathrm{D_{rc}} - (\mathrm{D_s} - \mathrm{h}') \quad (10)$$

where D_{rc} = depth of the road cut, D_s = soil depth, and $h' = h/\cos\alpha$. Variables h' and D_s are measured vertically for comparison to D_{rc} (Figure 3). When $h_{rc} > 0$, the predicted water table is above the base of the road cut, and subsurface flow interception by the road should occur, producing measurable runoff at the culvert. This approach would lead to an overestimation of water table elevation for partial equilibrium conditions (prior to steady state). This approach also neglects the drawdown effects of the seepage face on the water table [*Atkinson*, 1978], which may lead to overestimates of water table elevation in our calculations. This effect is likely small relative to other potential sources of error in the approach used here.

[26] Equations (4), (7), (9), and (10) were solved using values for site and storm conditions derived locally and from literature values (Table 3). Depth of the road cut, D_{rc}, and soil depth, D_s, were taken from measurements made in the field (Table 1). Hillslope length, X, for each subcatchment was measured manually from the digital elevation model as the distance from the road segment to the ridge measured perpendicular to the road, and average slope angle α for each subcatchment was determined by estimating slope for each grid cell on the digital elevation model using a standard GIS algorithm and computing the mean for the area of each subcatchment (Figure 2 and Table 1). A constant input rate was used in each calculation, and a range of timing and water table elevation estimates were generated for a range of input rates corresponding to average precipitation intensities of storms during the monitoring period (Tables 2 and 3). We adjusted our measurements of average precipitation intensities, r, slope length, X, and soil depth, Ds to compute values of i, L, and D used in the equations as follows:

$$\mathrm{i} = \mathrm{r}\cos\alpha \quad (11)$$

$$\mathrm{L} = \mathrm{X}/\cos\alpha \quad (12)$$

$$\mathrm{D} = \mathrm{D_s}\cos\alpha \quad (13)$$

2.7. Statistical Analyses

[27] Calculated estimates of response time and water table elevations were compared to observed runoff patterns by

road segment. Predicted and observed values were ranked, and rankings were compared visually or using correlation coefficients [*Ramsay and Schaefer*, 1997]. Linear regression models were fit to matched peak runoff events to assess the relationships between each instrumented subcatchment and WS3. The fitted regression models were used to predict peak runoff at subcatchments for a given peak runoff at WS3, and these predicted values from the empirical model were compared to the observed time to peak at instrumented culverts.

3. Results

[28] Ample precipitation during the monitoring period produced measurable runoff at most of the instrumented road segments in WS3. Runoff from the road segments was related to mapped characteristics of the subcatchments draining to each road segment, such as hillslope length, gradient, soil depth, and road cut depth as predicted by a simple model of hillslope flux. During large storm events, many road segments generated runoff that was synchronized with, and exceeded, the unit-area runoff in the 101-ha study catchment.

[29] The weather during the study period included conditions spanning the range of conditions for the entire period of record in this catchment. The 1995–96 water year was one of the wettest years in almost 45 years of record, producing over 30 storms in the five-month instrumented period (Table 2). Total annual precipitation recorded at Primet during water year 1996 exceeded 2900 mm, roughly 25% higher than average annual precipitation. The period from 1 October 1995 to mid-January 1996 was characterized by a series of moderate-intensity (<3 mm/hr), short to moderate-duration (15–81 hour) rain storms (Table 2). A period of snow accumulation began in mid-January and lasted approximately three weeks, bringing snow accumulation to 112% of the long-term water year average by early February. On 4 February, a warm, very humid storm system moved into the region, bringing a 3-day total rainfall exceeding 250 mm and melting much of the accumulated snowpack [*Marks et al.*, 1998]. On 6–7 February, this event produced the highest peak runoff measured in the 45-year record of small, low-elevation catchments at the Andrews Forest [*Swanson et al.*, 1998; *Jones*, 2000]. March and April were characterized by a series of low-intensity (<1.5 mm/hr) rain events with some snow accumulation.

[30] Subcatchments draining to the twelve instrumented road segments occupy 14% of the 101-ha WS3 (Table 1 and Figure 2). Instrumented road segments have contributing road surfaces ranging from 5 to 123 m^2 and contributing hillslopes ranging from <0.2 to just over 2.5 ha. Hillslopes contributing to instrumented road segments are steep, ranging from 25 to 72%. Soils are shallow, ranging in depth from only 0.25 m (C11) to over 4 m (C5, C7, C9, C13, C14), while cutbank depth ranges from 0 (C9, C13) to over 8 m (C1) (Table 1). Potential for interception of subsurface flow, as measured by the ratio of cutbank depth to soil depth, varied widely among road segments, from no potential for interception (C9, C13) to high potential for interception in cutbanks several times deeper than soils (C1, C2, C12, C16) (Table 1).

3.1. Observed Runoff From Mapped Areas Contributing to Roads

[31] Runoff from instrumented subcatchments ranged from quick flow to base flow-dominated (Figure 4). Runoff at C1, C2, C3 and C16 responded rapidly to precipitation and was synchronized with streamflow at WS3. Runoff responded more slowly to precipitation at C5, C7 and C14 and lagged behind WS3 peaks, although the runoff response was considerably more pronounced at C14 than at C5 and C7, which were largely driven by gradual changes in base flow. C13 responded similarly to C5 and C7 in timing, but the magnitude of runoff at C13 was considerably lower than at all other sites. No measurable runoff occurred at C9, C10 or C11 during the monitoring period. Gullying of the road surface and deposits of sediment and organic debris at the culvert inlets of C10 and C11 suggest that road surface runoff occurred during the February flood when the gaging instrumentation at these sites malfunctioned.

[32] Road surface runoff was a small fraction of measured runoff. Estimated road surface runoff accounted for 1% or less of the measured runoff at seven, and 3 to 7% at the other two, of the nine subcatchments where measurable runoff occurred (Table 1 and Figure 4). Roads in WS3 had not been graded for many years prior to the study, so much of the road surface was deeply rutted, and precipitation was held in depression storage or discharged to hillslopes below the road without passing through the drainage ditch and culvert. For most road segments, the contributing road surface included only the inboard section of the crowned road surface and, in some cases, only the inboard ditch on deeply rutted road segments, producing road surface contributing areas of only 5 to 50 m^2 (Table 1). Two road segments had larger contributing areas (100 to 123 m^2) involving wheel ruts extending up the road beyond the adjacent culvert. Recession limbs of measured hydrographs extend tens of hours beyond cessation of rainfall (Figure 4), suggesting that runoff is produced from sources other than intercepted precipitation on the road surface.

3.2. Comparisons to Theoretical Predictions

[33] Theoretical predictions of response lags illustrate the role of storm and site conditions in influencing the timing of runoff response (Figure 5). For average rainfall rates ranging from less than 1 to 5 mm/hr, predictions of unsaturated zone response time (Tuz) range from 50 to 350 hours under assumptions of very dry initial conditions and from only 20 to 40 hours under assumptions of very wet initial conditions under one hillslope scenario (Figure 5a). For soil depths ranging from less than one meter to 5 m, predicted unsaturated zone response times range from 50 to nearly 400 hours under assumptions of very dry initial conditions and from less than 20 to 40 hours under assumptions of very wet initial conditions for one hillslope/input rate scenario (Figure 5b). Similarly, predicted saturated zone response times (Tc) range from 100 to 300 hours at low intensity (0.5 mm/hr) precipitation but range from 30 to 80 hours at high (5 mm/hr) precipitation rates over the range of slope lengths and hillslope gradients characteristic of our sites (Figures 5c and 5d). Comparison of these timing predictions to runoff hydrographs from the culverts suggests that our sites peak prior to steady state on these hillslopes. Predicted times to equilibrium calculated under assumptions of very wet antecedent conditions for very high rainfall rates (Table 4) exceed observed times to peak, which range from 9 to 63.5 hours, on the instrumented road segments (Table 5).

[34] Estimates of timing based on the kinematic model help explain observed patterns of runoff timing at instru-

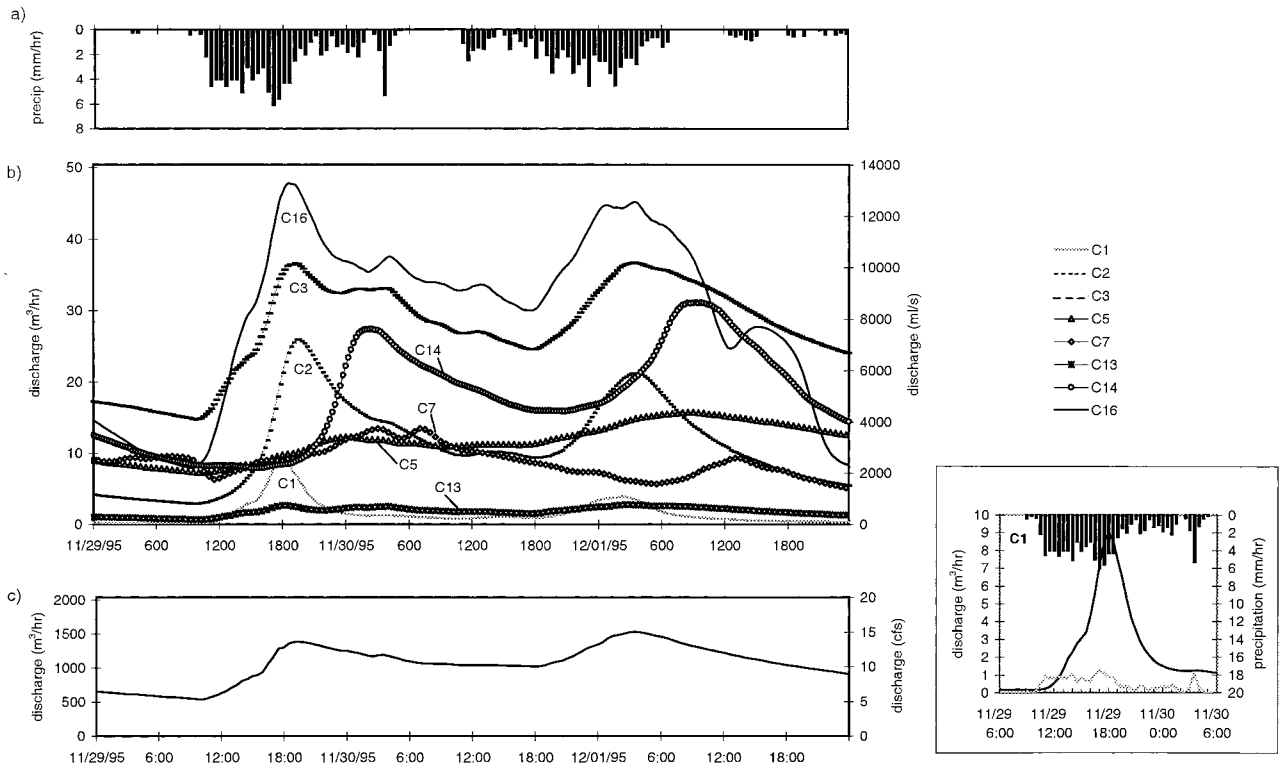

Figure 4. (a) Precipitation hyetograph and storm hydrographs from (b) instrumented culverts and (c) WS3, 29 November to 1 December 1995. Inset shows 29 November storm for C1 with total measured runoff graphed as black line and estimated road surface runoff (from equation 1, using 15-min precipitation series) graphed as shaded line.

mented road segments. In general, our calculations for time to equilibrium predict rapid response at C1, C2 and C16 and slow response at C5, C7 and C13 (Table 4). Observed times to peak under presumably partial equilibrium conditions follow this pattern rather closely, with peaks occurring earliest at C1, C2 and C16 for most storms and late at C5 and C7 (Table 5). The very short observed times to peak at C13 for storms between 27 and 30 November occur as a result of low flow variability at this site, and may be a result of road surface runoff rather than subsurface flow interception. Observed time to peak was longest both for storms of long precipitation duration (24 November and 28 December) and for late season storms (18 January), when soil moisture conditions were presumably very wet (Table 5). This finding, in contrast to our expectation of short response times for wet antecedent conditions, suggests that the effective slope length producing runoff may expand through the season.

[35] The ordering of runoff timing on the instrumented road segments was not consistent among sites across all storms, an observation that is corresponds to our predictions. The ordering of predicted unsaturated zone response times differs from the ordering of predicted saturated zone response times, reflecting variations in soil depth, slope length, and slope gradient across the sites (Table 4). Changes in the timing of unsaturated zone response under different assumptions of initial moisture conditions also leads to differences in the ordering of predicted times to equilibrium (Table 4). These predictions suggest that across a range of storm events with differing antecedent conditions and precipitation rates, the ordering of observed runoff timing among our sites will vary, a pattern that we see in our observations of time to peak for the road segments (Table 5). For example, C1 peaks before C16 for all but the storm of 28 December, and C2 peaks before or simultaneously with C3 for all but the storm of 30 November. Similarly C14 peaks before C7 for all but the storm of 18 January, and C5 peaks before C14 for all but the storm of 28 December. The greatest differences in the ordering of time to peak occur between the storm of 24 November and 18 January, when the greatest differences in antecedent conditions would be expected to exist.

[36] Instrumented road segments that produced measurable runoff were consistent with those predicted to have a water table intercepted by the road cut, even under the presumably transient conditions evident at these sites. Only some road segments were predicted to produce runoff through interception of a hillslope water table (Figure 6). Interception of subsurface flow was predicted to occur over the entire range of precipitation intensities at C1, C2, C3, and C16, but not at C9, C10, C11, and C13. Subsurface flow interception and runoff were predicted to occur at C5, C7, and C14 above a threshold of precipitation intensity ranging from 0.5 to 3.25 mm/hr. Observed thresholds of runoff response followed predictions rather closely (Figure 7). C16 produced runoff during all but one rain event and two rain-on-snow or mixed events. As predicted, C9, C10, and C11 failed to produce runoff by subsurface flow interception. Runoff exhibited a threshold response at C5, C7, C14 and at C1, C2, C3 and C13. Average precipitation intensity and total storm precipitation depth interacted to produce runoff on these sites.

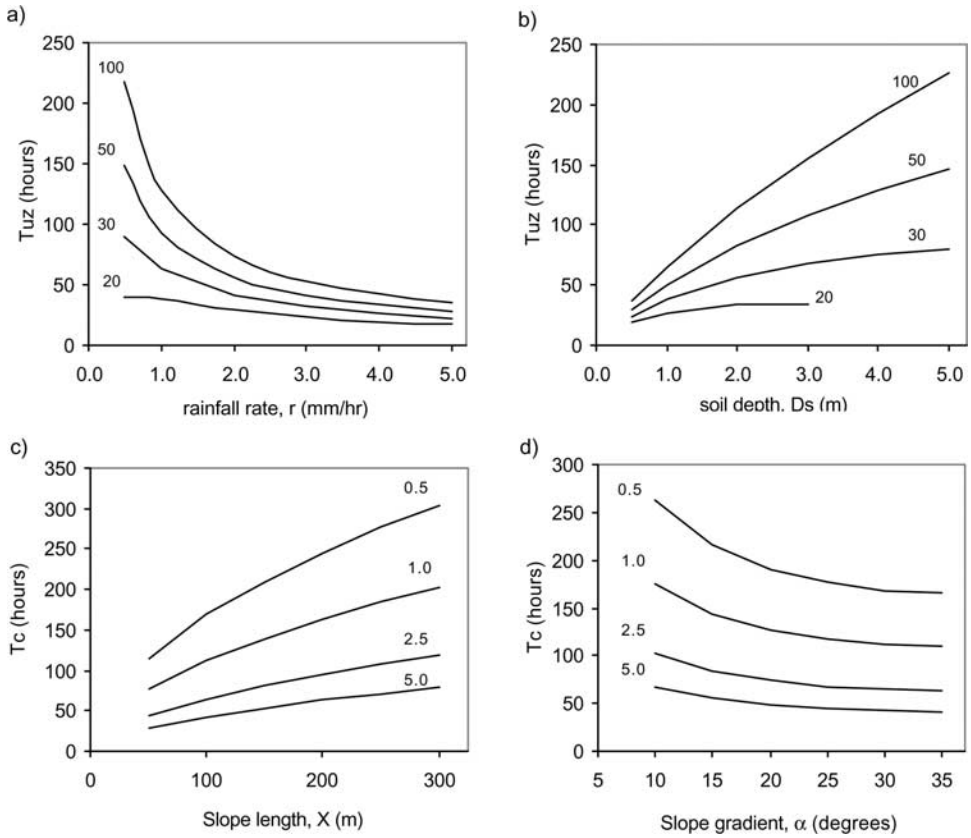

Figure 5. Predictions of unsaturated zone timing (Tuz) under initial moisture conditions ranging from ψ_o = 20 to 100 cm and saturated zone timing (Tc) under rainfall conditions ranging from r = 0.5 to 5 mm/hr (i varies with slope gradient) for four scenarios: (a) D_s = 1 m, X = 100 m, α = 30°, (b) i = 2 mm/hr, X = 100 m, α = 30°, (c) D_s = 1 m, α = 30°, and (d) D_s = 1 m, X = 100 m.

[37] The pattern of cumulative runoff over the monitoring period for each road segment is consistent with estimates from the kinematic model, despite likely discrepancies between observed and predicted patterns of runoff, due to transient runoff behavior not captured in our steady state predictions and to differences in base flow and quick flow production among subcatchments (Figure 4). If the duration of water table rise above the base of the road cut were the only factor influencing cumulative runoff, the predicted ranking of water table elevation relative to the road cut (Figure 6) should correspond to the predicted ranking of cumulative runoff (Figure 8). These rankings agree rather closely (r = 0.76). Predictions of cumulative runoff patterns using this simple assumption were poorest for C5 (predicted rank 7, observed rank 1) and C1 (predicted rank 4, observed rank 7). The lower than predicted cumulative runoff at C1 reflects the rapid storm flow recession in the subcatchment contributing to this road segment (Figure 4), while the higher than predicted cumulative runoff at C5 reflects the sustained base flow response at this site. Subcatchments dominated by a base flow contribution to the road segment (e.g., C5, C7) produced more cumulative runoff than subcatchments dominated by a quick flow contribution to the road segment (e.g., C1, C2) (Figure 4).

3.3. Comparisons to Catchment Response

[38] Unit area peak runoff from instrumented subcatchments contributing to road segments were positively related to unit area peaks at WS3, and exceeded them during large storm events in a majority of subcatchments (Figure 9). Of the eight instrumented subcatchments whose peak runoff events could be matched with peaks at WS3, seven had unit area peaks that were strongly positively related to the peak at WS3 (r^2 values from 0.51 to 0.97). Four subcatchments

Table 4. Predictions of Time of Unsaturated Zone Response (Tuz), Time of Concentration (Tc), and Time to Equilibrium (Te) and Rank of Timing Response Under Three Scenarios With Different Assumptions of Initial Soil Moisture Conditions for Sites With Measurable Runoff[a]

		Very Wet (ψ_o = 20 cm)		Intermediate (ψ_o = 30 cm)		Dry (ψ_o = 50 cm)	
	Tc	Tuz	Te	Tuz	Te	Tuz	Te
C1	28.4 *(1)*	14.5 *(2)*	42.9 *(1)*	22.6 *(2)*	51.0 *(1)*	27.7 *(2)*	56.1 *(1)*
C2	59.0 *(3)*	21.0 *(3)*	80.0 *(2)*	37.5 *(3)*	96.5 *(3)*	48.1 *(3)*	107.1 *(3)*
C3	70.5 *(6)*	23.9 *(4)*	94.4 *(7)*	46.2 *(4)*	116.7 *(4)*	60.5 *(4)*	131.0 *(4)*
C5	63.8 *(5)*	29.2 *(7)*	93.0 *(5)*	63.0 *(7)*	126.8 *(6)*	84.8 *(7)*	148.6 *(6)*
C7	59.8 *(4)*	33.3 *(8)*	93.1 *(6)*	102.5 *(8)*	162.3 *(8)*	147.0 *(8)*	206.8 *(8)*
C13	82.6 *(8)*	27.0 *(5)*	109.6 *(8)*	60.9 *(5)*	143.5 *(7)*	82.8 *(5)*	165.4 *(7)*
C14	57.9 *(2)*	28.0 *(6)*	85.9 *(4)*	61.9 *(6)*	119.8 *(5)*	83.7 *(6)*	141.6 *(5)*
C16	71.4 *(7)*	11.0 *(1)*	82.4 *(3)*	16.2 *(1)*	87.6 *(2)*	19.6 *(1)*	91.0 *(2)*

[a]Tc is unaffected by initial moisture conditions and remains constant across three scenarios. Input rate used in these calculations is equivalent to an average precipitation rate of 5 mm/hr. Rank of timing response is in italics.

Table 5. Time to Peak and Rank of Timing for Nine Storms at Sites With Measurable Runoff[a]

	24 Nov. 1995 69 hours	27 Nov. 1995 34 hours	29 Nov. 1995 20 hours	30 Nov. 1995 23.5 hours	8 Dec. 1995 32.5 hours	28 Dec. 1995 70 hours	7 Jan. 1996 24 hours	14 Jan. 1996 73.5 hours	18 Jan. 1996 35 hours	Minimum	Maximum	Mean
C1	34.75 *(1)*		9.00 *(1)*	19.00 *(1)*	25.75 *(1)*	51.00 *(2)*	13.75 *(1)*	19.00 *(1)*	20.50 *(1)*	9.00	51.00	24.09 *(1)*
C2	38.00 *(3)*		10.25 *(4)*	20.25 *(4)*	29.25 *(3)*	51.50 *(3)*	17.25 *(3)*	31.25 *(2)*	25.50 *(2)*	10.25	51.50	27.91 *(2)*
C3	48.00 *(6)*		10.25 *(4)*	20.00 *(3)*	30.75 *(4)*	51.75 *(4)*	17.75 *(4)*	50.50 *(3)*	37.50 *(3)*	10.25	51.75	33.31 *(5)*
C5	41.50 *(4)*		15.00 *(5)*	25.75 *(5)*		56.00 *(7)*				15.00	56.00	34.56 *(6)*
C7	51.25 *(8)*		18.00 *(7)*	30.00 *(7)*	52.25 *(7)*	59.25 *(6)*	35.75 *(6)*	58.00 *(4)*	44.50 *(4)*	18.00	59.25	43.62 *(8)*
C13	48.25 *(7)*	20.50 *(2)*	9.25 *(2)*	19.50 *(2)*	37.50 *(5)*				62.75 *(6)*	9.25	62.75	32.96 *(4)*
C14	43.25 *(5)*	20.50 *(2)*	17.00 *(6)*	26.00 *(6)*	38.50 *(6)*	54.25 *(5)*	24.50 *(5)*		63.50 *(7)*	17.00	63.50	35.94 *(7)*
C16	36.25 *(2)*	20.00 *(1)*	9.50 *(3)*	20.25 *(4)*	26.50 *(2)*	48.75 *(1)*	14.50 *(2)*		51.50 *(5)*	9.50	51.50	28.41 *(3)*
Minimum	34.75	20.00	9.00	19.00	25.75	48.75	13.75	19.00	20.50			
Maximum	51.25	20.50	18.00	30.00	52.25	59.25	35.75	58.00	63.50			
Mean	42.66	20.33	12.28	22.59	34.36	53.21	20.58	39.69	43.68			

[a]Time to peak is defined as time from beginning of rainfall to peak of the runoff hydrograph. Duration of precipitation event in hours is given below each storm date. Rank of timing is given in italics.

(C1, C7, C14, and C16) consistently produced unit-area peak runoff exceeding the unit-area peak at WS3, and two (C2 and C3) produced higher unit-area peaks than WS3 for events exceeding 1 mm/hr at WS3. C5 and C13 consistently produced unit-area peak runoff less than the unit peak at WS3.

[39] Road segments with shorter observed times to peak produced higher unit-area peak runoff. Peak runoff at subcatchments ranged from 1 to 4 mm/hr for a unit-area peak of 1.5 mm/hr at WS3 based on empirical models in Figure 9. These peak runoff rates declined as the observed time to peak increased, but this relationship was not statistically significant (Figure 10).

[40] Peak runoff from instrumented subcatchments contributing to road segments became increasingly synchronized with the peak runoff at WS3 as event size increased (Figure 11). Peaks from most subcatchments occurred after the peak at WS3 for most storms; however, peaks at C1 and C16 consistently preceded the peak at WS3 (Figure 11). For the four largest events, peak runoff from subcatchments occurred between 3 hours before the peak at WS3 and 8 hours after the peak at WS3. Considering that the duration of storm hydrographs for events of this size at WS2 (control catchment matched with WS3) exceeds 90 hours [*Perkins*, 1997; R. M. Perkins and J. A. Jones, manuscript in preparation, 2003], this represents fairly close synchronization.

[41] Road segments whose culverts discharged near channel heads (in the sense of *Montgomery and Dietrich* [1988]) were more likely to contribute significant fractions of the peak at WS3, and to be timed to contribute to the early part of the peak at WS3 (Figures 11 and 12). For a set of nine storms over the period from 25 November through 20 January, five instrumented subcatchments (C2, C3, C5, C14, and C16) consistently dominated storm runoff production from road segments. During several of these storms, these subcatchments generated peak runoff rates amounting to 5 or 10% of the peak at WS3, despite having drainage areas less than 2.5% of the area of WS3. Peaks from C2, C3, and C16 were synchronized with or preceded the peak at WS3 (Figure 11).

4. Discussion

[42] Our findings indicate that the production of runoff on roads in steep forest lands is influenced by variable storm conditions and by mappable characteristics of the subcatchments draining to each road segment and suggest that runoff produced on some road segments may alter the timing and magnitude of hydrographs at the catchment scale. Interception of subsurface flow accounted for over 95% of measured runoff from subcatchments contributing to road segments in WS3, a steep mountain watershed in the Andrews Forest in western Oregon. The interception of subsurface flow along road segments corresponded reasonably well with estimates of precipitation intensity required for the water table to rise above the base of the road cut. The timing of peak runoff from subcatchments draining to road segments varied according to characteristics of the storm, including precipitation rates and antecedent conditions. Runoff from key road segments may augment the rising limb of the catchment-wide storm hydrograph during storm events. Subcatchments with shorter response times had consistently higher unit area peaks than those with longer response times. As the size of the peak increased at WS3, runoff from subcatchments draining to road segments became

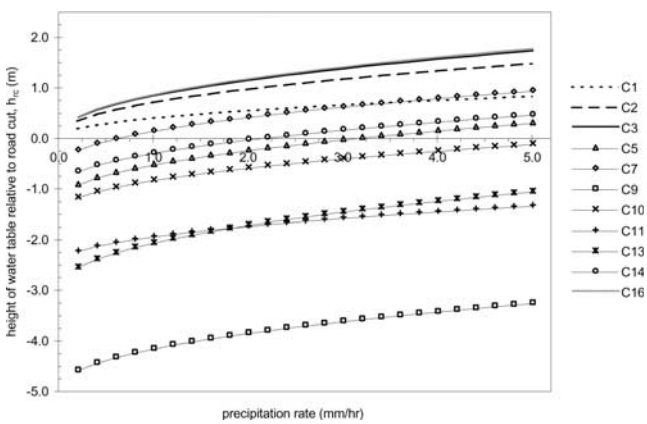

Figure 6. Predictions of water table elevation relative to the road cut (h_{rc}, using equation 10) for instrumented road segments in WS3 at the Andrews Experimental Forest. The predicted ranking of h_{rc} from highest to lowest is as follows: C16, C3, C2, C1, C7, C14, C5, C10, C13, C11, and C9. (note h_{rc} at C7 exceeds h_{rc} at C1 for calculations with precipitation rate > 4 mm/hr and h_{rc} at C13 is less than h_{rc} at C11 for calculations with precipitation rate < 1.5 mm/hr).

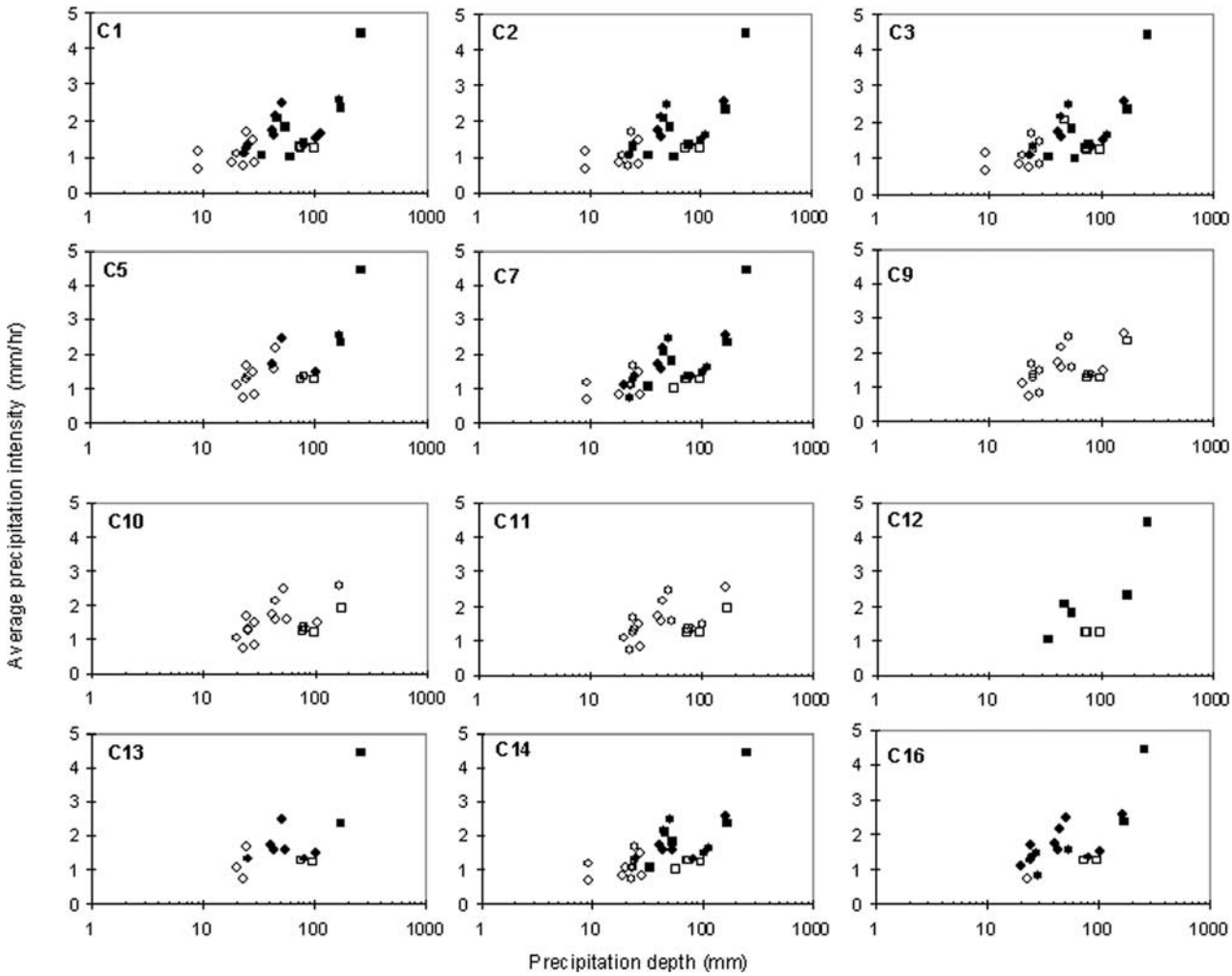

Figure 7. Plots of average precipitation intensity versus precipitation depth for storms between 16 November 1995 and 21 April 1996 at instrumented subcatchments. Circles represent rain events, squares represent snow and mixed rain-snow events. Solid symbols represent precipitation events that produced measurable runoff at instrumented sites. Open symbols represent precipitation events that did not produce detectable storm runoff. Plot for each site includes all precipitation events for which runoff monitoring occurred (see Table 1).

increasingly synchronized with the peak at the mouth of the watershed. Subcatchments draining to road segments near channel heads contributed runoff peaks with unit-area runoff rates several times higher than those at WS3 and timed to contribute to the rising limb of the WS3 storm hydrograph.

[43] Differences in hydrologic behavior among segments of a road network observed in this study are attributable to the position of each road segment relative to hydrologic flow paths. The distance between each road segment and the ridge above interacts with variations in the ratio of road cut depth to soil depth to produce predictably different responses among adjacent segments of the same road. Controlling for hillslope length, road segments whose road cuts intersected the entire soil profile were more likely to produce runoff than road segments whose road cuts intersected only part of the soil profile. Road segments draining short slopes with shallow soils were more likely than other road segments to produce rapid runoff response, timed to coincide with, or precede, the peak at the mouth of WS3. Runoff-producing subcatchments in this study ranged from 0.2 to 2.5 ha (Table 1), mostly below the threshold for channel initiation in the wettest conditions, which is estimated at 2 ha [*Wemple et al.*, 1996]. Thus the presence of roads appears to reduce the threshold for channel initiation by intercepting subsurface flow paths in an artificial subcatchment comprising the hillslope above the road cut, the road surface, and the ditch. This effect might be expected to change seasonally as the variable source area for channel initiation expands and contracts. During the flood of February 1996 and again during flooding in November 1996, the hillslope above C3 developed channelized overland flow. The channel mapped at C16 (Figure 1) flows intermittently. During large storms these sites may have little effect on rearranging preexisting flow paths.

[44] Despite its relative utility in predicting road segment behavior, the theoretical model used in this study does not capture potentially important aspects of hillslope-scale hydrologic behavior in WS3 and similar steep catchments. It is probable that subsurface flow paths in subcatchments of

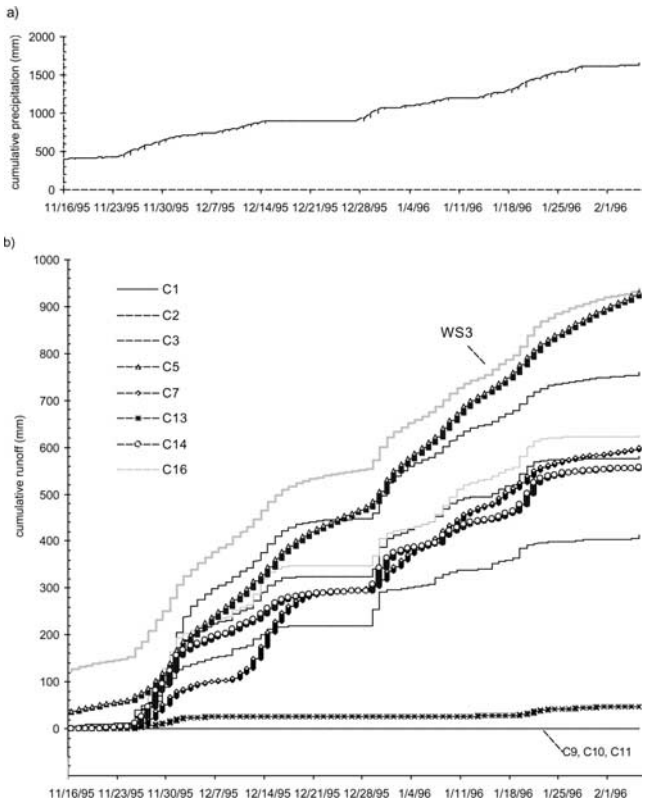

Figure 8. Cumulative (a) precipitation and (b) unit-area runoff for 11 road segments (excluding C12 where monitoring did not begin until mid-January 1996) and WS3 from 16 November 1995 through 4 February 1996. The observed ranking of cumulative runoff for the road segments, from highest to lowest, is as follows: C5, C3, C16, C2, C7, C14, C1, C13, C10 = C11 = C9 (note cumulative runoff at C7 exceeds C2 after 25 January 1996).

WS3 are influenced by surface topographic convergence evident on many of the hillslopes draining to our instrumented road segments. Effective slope lengths producing runoff may be shorter than the full length of the hillslope from ridge to road cut, as recognized in previous studies (see discussion by *Beven* [1982a]). Bedrock topography may also influence subsurface flow patterns as shown in small, steep catchments elsewhere [*McDonnell*, 1996]. Topographic convergence would have the effect of raising the hillslope water table and enhancing the effect of subsurface flow interception by roads beyond that which is captured by the simple 2D model applied here. Shorter effective slope lengths than those represented by our mapped estimates would be expected to produce more rapid runoff than our calculations predict. Finally, bedrock topography that does not correspond to surface topography would be expected to produce observed patterns of runoff that correspond poorly to predicted patterns based on this model. Beyond the possible errors introduced by inadequate representation of hillslope geometry, preferential flow through macropores and hillslope colluvium observed at our sites during large storm events is not represented in our predictions. We propose that the simple theoretical model applied here is most useful for examining the relative importance of differences in hillslope geometry and road configuration on the magnitude and timing of runoff production among segments of forest roads constructed on steep hillslopes.

[45] Additional field studies, experimental work, and modeling to understand hydrology of steep hillslopes may be usefully conducted in catchments with roads. Hillslopes in WS3 probably resemble nearby WS10, where preferential flow occurs in ephemeral, discontinuous saturated zones not continuously linked to stream channels [*Harr*, 1977]. Small catchments with roads, such as WS3, would be instructive field sites in which to pursue the debate about the role of surface and subsurface topographic effects on flow in hillslopes [*Woods and Rowe*, 1996; *McDonnell*, 1997]. Tracer and flow path studies might elucidate the complex issue of preferential flow path geometry [*Ziemer and Albright*, 1987; *Tsuboyama et al.*, 1994] and the role of roads in enhancing connectivity of subsurface and surface flow paths where macropore flow occurs. Experimental road removal or a catchment-scale trenching experiment could be devised to test whether road modification of hillslope flow paths influences the catchment-scale hydrograph. In contrast to the simple calculations used in this study, several recent studies have used more computationally sophisticated simulation models to represent the dynamics of subsurface flow interception by roads [*Dutton*, 2000; *Bowling and Lettenmeier*, 2001; *Tague and Band*, 2001; *Wigmosta and Perkins*, 2001]. These models build on earlier attempts to simulate overland flow and runoff on road surfaces in forested environments [*Cundy and Tento*, 1985; *Luce and Cundy*, 1992, 1994]. Output from these models could be sampled at the subcatchment scale used in this study, to test whether they reproduce the observed differences in runoff between adjacent road segments of WS3.

[46] This study shows that road segments may interact in at least four distinct ways with complex landforms in forested terrain, potentially producing very different effects depending on landform characteristics. Road segments on the easternmost portions of WS3 intercepted subsurface flow from short, steep slopes (Figures 2 and 12 and Table 1), producing storm hydrographs timed to contribute to the earliest, highest portion of the catchment-wide storm hydrograph. Other road segments whose cutbank depth was a smaller fraction of the soil depth (C5, C7 in Table 1) produced primarily base flow and contributed only to the falling limb of the catchment-wide storm hydrograph. Still other culverts in the western portion of WS3 (Figures 2 and 12) were constructed on large slump benches and never produced measurable runoff. Finally, most of the subcatchments formerly drained by roads in the western portion of WS3 (Figure 2) could not be instrumented, because mass movements from these roads shortly after their construction led to road abandonment and culvert removal in the 1960s. In general, road network effects on catchment hydrology and geomorphology in landscapes with deep flow paths may resemble those observed in the western portion of WS3, with little long-term effect of roads on storm hydrographs. On the other hand, road networks in landscapes with steep gradients and shallow flow paths may resemble those observed in the eastern portion of WS3, with persistent effects on storm hydrographs and debris flow potential.

[47] Restoration targeted at road segments predicted to be hydrologically and geomorphically important might reduce

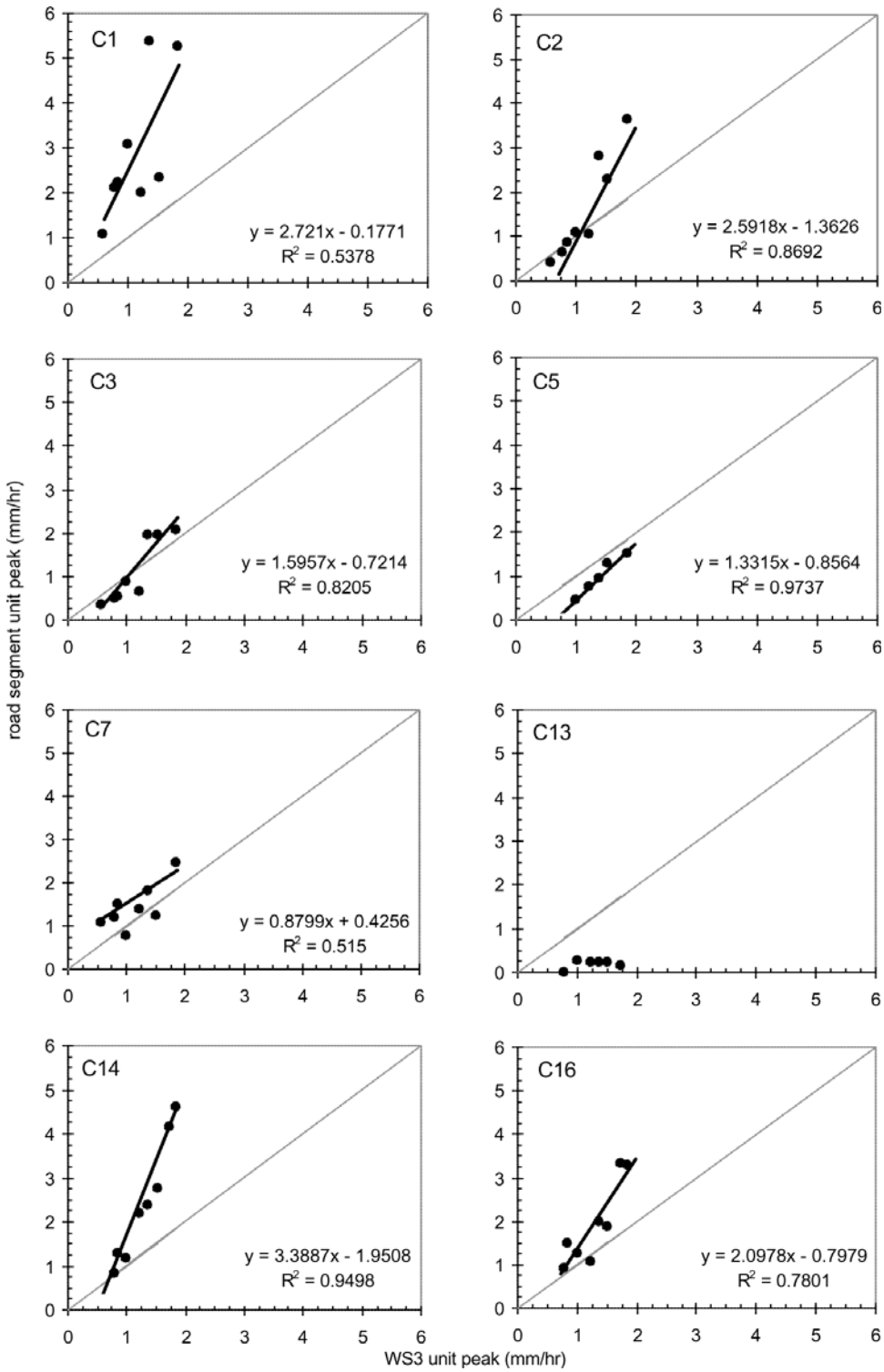

Figure 9. Relationships fitted with linear regression between unit area peak runoff in eight subcatchments draining to road segments and the matched peak runoff at WS3. Thin shaded line is 1:1. Points are storms between November 1995 and February 1996 for which road segment hydrographs could be matched with WS3 hydrographs.

both the hydrologic and geomorphic hazards of forest roads in steep landscapes. In this study only a few road segments were responsible for a large proportion of the inferred hydrologic effects of roads. Moreover, key road segments in WS3 that intercepted subsurface flow (e.g., C5, C12 and C16) are in locations that produced debris flows in 1960s and 1996 [*Fredriksen*, 1970; *Swanson and Dyrness*, 1975; *Snyder*, 2000; *Wemple et al.*, 2001]. The techniques developed in this study, which predict the relative potential for runoff generation by road segments, might be used to

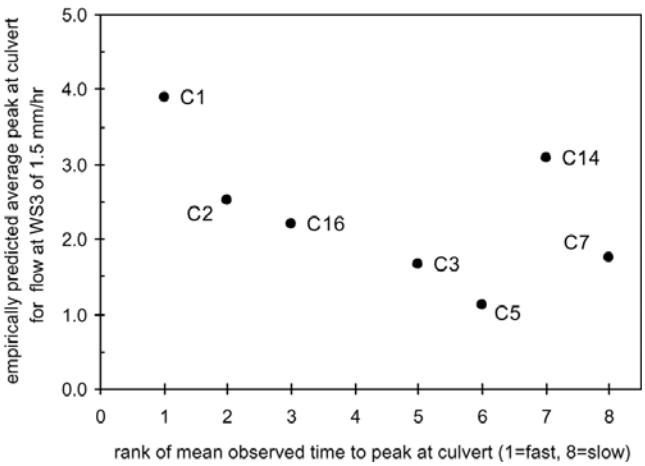

Figure 10. Relationship between unit-area peak runoff at subcatchments draining to road segments, predicted from empirical relationships in Figure 9, and the rank of mean time to peak, from Table 5, for sites producing measurable runoff. C7 is not plotted since unit area peak at the site cannot be predicted from the WS3 peak discharge.

prioritize road segments for restoration activities. Application of this approach at other sites however would require sufficiently detailed topographic data to delineate road catchments and accurate estimates of soil depth and road cut depth along a road network. Computer algorithms could be used to estimate road cut depth, given basic assumptions about road design [*Wigmosta and Perkins*, 2001], potentially automating the process and providing first-cut estimates of model parameters for extensive road networks.

[48] Road restoration to reduce runoff from subsurface flow interception by roads involves tradeoffs with other road restoration objectives such as control of fine sediment delivery to streams or mass movements associated with roads. Road restoration techniques, which range from minor modifications of the road surface to partial or complete road pullback, have a wide range of long-term consequences [*Madej*, 2001]. Of these techniques, hillslope recontouring would be most likely to modify subsurface flow pathways in such a way as to influence downstream peak runoff. In contrast, modifications of road surface drainage (such as by ripping the road surface or diverting flow with water bars) would be expected to have relatively little effect on downstream peaks in catchments where road runoff is dominated by subsurface flow interception. Road surface runoff was a minor component of road runoff in this study, but it can have disproportionately large geomorphic and ecological consequences. Road surface modifications might prevent a range of road-drainage-related geomorphic effects, including destabilization of the fill slope [*Swanson and Dyrness*, 1975], fine sediment delivery [e.g., *Reid*, 1981; *Reid and Dunne*, 1984], and blocked culverts and their cascading fluvial and mass wasting effects [*Wemple et al.*, 2001].

[49] Overall, the findings of this study are consistent with the hypothesis that some road segments intercept subsurface flow, route it to ditches and thence directly to streams, and thereby alter the overall timing of water delivery in the catchment [*King and Tennyson*, 1984; *Jones and Grant*, 1996]. Moreover, during the largest peak runoff events,

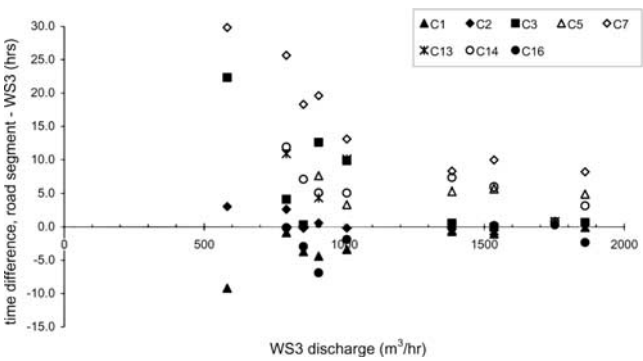

Figure 11. Plot of time difference between road segment and catchment peak runoff versus WS3 runoff rate for storms between November 1995 and February 1996 at 8 road segments that produced measurable runoff. Points are storms between November 1995 and February 1996 for which road segment hydrographs could be matched with WS3 hydrographs.

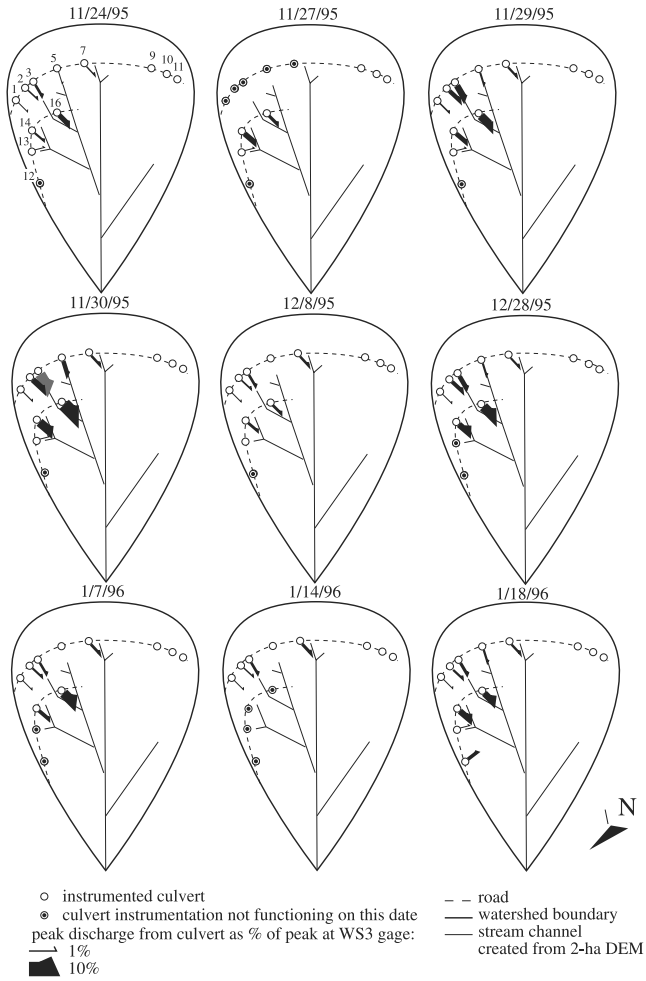

Figure 12. Spatial arrangement of subcatchment contributions to peak runoff at WS3 for a series of storm events from November 1995 to early January 1996. Each arrow represents the peak runoff from a subcatchment draining to a road segment with the width of the arrow scaled as a percentage of the peak runoff at WS3.

segments of the road network in WS3 were increasingly able to produce runoff that contributed to the rising limb of the storm hydrograph. Thus only a small portion of the road network might contribute to flood augmentation. Future studies should examine the emergent behavior of extensive road networks, especially during large storm events, to determine how road networks alter runoff production and routing, and thereby potentially contribute to increased downstream flooding.

[50] **Acknowledgments.** This work was supported through funding from the U. S. Geological Survey, Biological Resources Division (grant H952-A1-0101-19), and the National Science Foundation (grant DEB 96-32921 to the Long-Term Ecological Research Program at the H. J. Andrews Experimental Forest). We thank A. Levno, C. Creel and G. Downing for assistance with site instrumentation; C. Luce for guidance on instrumentation design; D. Henshaw for access to meteorological and streamflow data from the Andrews Forest, and J. Means for the Lidar imagery used to create the digital elevation map of Watershed 3. K. Beven, J. McDonnell, R. Perkins, F. Swanson and two anonymous reviewers provided helpful comments on the manuscript. The data compiled for this study are available by request through the Forest Science databank, maintained by the H. J. Andrews LTER Program (http://www.fsl.orst.edu/lter).

References

Anderson, M. G., Road-cut slope topography and stability relationships in St. Lucia, West Indies, *Applied Geography*, *3*, 104–114, 1983.

Anderson, M. G., and T. P. Burt, The role of topography in controlling throughflow generation, *Earth Surf. Processes*, *3*, 331–344, 1978.

Atkinson, T. C., Techniques for measuring subsurface flow on hillslopes, in *Hillslope Hydrology*, edited by M. J. Kirkby, pp. 73–120, John Wiley, Hoboken, N. J., 1978.

Beschta, R. L., M. R. Pyles, A. E. Skaugset, and C. G. Surfleet, Peakflow responses to forest practices in the western cascades of Oregon, USA, *J. Hydrol.*, *233*, 102–120, 2000.

Beven, K., On subsurface stormflow: An analysis of response times, *Hydrol. Sci. J.*, *4*, 505–521, 1982a.

Beven, K., On subsurface stormflow: Predictions with simple kinematic theory for saturated and unsaturated flows, *Water Resour. Res.*, *18*, 1627–1633, 1982b.

Bowling, L. C., and D. P. Lettenmeier, Evaluation of the effects of forest roads on flood flows in a mountainous maritime environment, in *Land Use and Watersheds: Human Influence on Hydrology and Geomorphology in Urban and Forest Areas*, *Water Sci. Appl. Ser.*, vol. 2, edited by M. Wigmosta and S. Burgess, pp. 145–164, AGU, Washington, D. C., 2001.

Croke, J., and S. Mockler, Gully initiation and road-to-stream linkage in a forested catchment, southeastern Australia, *Earth Surf. Processes Landforms*, *26*, 205–217, 2001.

Cundy, T. W., and S. W. Tento, Solution to the kinematic wave approach to overland flow routing with rainfall excess given by Philip's equation, *Water Resour. Res.*, *21*, 1132–1140, 1985.

Dunne, T., T. R. Moore, and C. H. Taylor, Recognition and prediction of runoff-producing zones in humid regions, *Hydrol. Sci. Bull.*, *20*, 305–327, 1975.

Dutton, A. L., Process-based simulations of near-surface hydrologic response for a forested upland catchment: the impact of a road, M.S. thesis, 151 pp., Stanford Univ., Stanford, Calif., 2000.

Dyrness, C. T., Hydrologic properties of soils on three small watersheds in the western Cascades of Oregon, *Res. Note PNW-111*, Pac. Northwest For. and Range Exp. Stn., U.S. For. Serv., Corvallis, Oreg., 1969.

Fredriksen, R. L., Erosion and sedimentation following road construction and timber harvest on unstable soils in three small western Oregon watersheds, *Res. Pap. PNW-104*, Pac. Northwest For. and Range Exp. Stn., U.S. For. Serv., Corvallis, Oreg., 1970.

Grant, G. E., and A. L. Wolff, Long-term patterns of sediment transport after timber harvest, western Cascade mountains, Oregon, USA, in *Sediment and Stream Water Quality in a Changing Environment: Trends and Explanation*, *IAHS Publ.*, *203*, 31–40, 1991.

Greenland, D., The Pacific Northwest regional context of the climate of the H. J. Andrews experimental forest long-term ecological research site, *Northwest Sci.*, *69*, 81–96, 1994.

Harr, R. D., Water flux in soil and subsoil on a steep forested slope, *J. Hydrol.*, *33*, 37–58, 1977.

Harr, R. D., Some characteristics and consequences of snowmelt during rainfall in western Oregon, *J. Hydrol.*, *53*, 277–304, 1981.

Janda, R. J., K. M. Nolan, D. R. Harden, and S. M. Colman, Watershed conditions in the drainage basin of Redwood Creek, Humboldt County, California as of 1973, *U.S. Geol. Surv. Open File*, *75-568*, 1975.

Jones, J. A., Hydrologic processes and peak discharge response to forest removal, regrowth, and roads in 10 small experimental basins, western Cascades, Oregon, *Water Resour. Res.*, *36*, 2621–2642, 2000.

Jones, J. A., and G. E. Grant, Peak flow responses to clear-cutting and roads in small and large basins, western Cascades, Oregon, *Water Resour. Res.*, *32*, 959–974, 1996.

Jones, J. A., and G. E. Grant, Comment on "Peak flow responses to clear-cutting and roads in small and large basins, western Cascades, Oregon: A second opinion" by R. B. Thomas and W. F. Megahan, *Water Resour. Res.*, *37*, 175–178, 2001.

King, J. G., and L. C. Tennyson, Alteration of streamflow characteristics following road construction in north central Idaho, *Water Resour. Res.*, *20*, 1159–1163, 1984.

Luce, C. H., Hydrological processes and pathways affected by forest roads: What do we still need to learn?, *Hydrol. Processes*, *16*(14), 2901–2904, 2002.

Luce, C. H., and T. W. Cundy, Modification of the kinematic wave-Philip infiltration overland flow model, *Water Resour. Res.*, *28*, 1179–1186, 1992.

Luce, C. H., and T. W. Cundy, Parameter identification for a runoff model for forest roads, *Water Resour. Res.*, *30*, 1057–1069, 1994.

Madej, M. A., Erosion and sediment delivery following removal of forest roads, *Earth Surf. Processes Landforms*, *26*, 175–190, 2001.

Marks, D., J. Kimball, D. Tingey, and T. Link, The sensitivity of snowmelt processes to climate conditions and forest cover during rain-on-snow: A case study of the 1996 Pacific Northwest flood, *Hydrol. Processes*, *12*, 1569–1587, 1998.

McDonnell, J. J., Comment on "The changing spatial variability of subsurface flow across a hillside" by R. Woods and L. Rowe, *J. Hydrol. N. Z.*, *36*, 103–106, 1997.

McDonnell, J. J., J. Freer, R. Hooper, C. Kendall, D. Burns, K. Beven, and J. Peters, New method developed for studying flow on hillslopes, *Eos Trans. AGU*, *77*, 465, 472, 1996.

Megahan, W. F., Subsurface flow interception by a logging road in mountains of central Idaho, paper presented at National Symposium on Watersheds in Transition, Colo. State Univ., Fort Collins, 1972.

Megahan, W. F., and J. L. Clayton, Tracing subsurface flow on roadcuts on steep, forested slopes, *Soil Sci. Soc. Am. J.*, *47*, 1063–1067, 1983.

Megahan, W. F., and W. J. Kidd, Effect of logging roads on sediment production rates in the Idaho batholith, *Res. Pap. INT-123*, Intermt. For. and Range Exp. Stn., U.S. For. Serv., Ogden, Utah, 1972.

Montgomery, D. R., Road surface drainage, channel initiation, and slope instability, *Water Resour. Res.*, *30*, 1925–1932, 1994.

Montgomery, D. R., and W. E. Dietrich, Where do channels begin?, *Nature*, *336*, 232–234, 1988.

Montgomery, D. R., and W. E. Dietrich, Hydrologic processes in a low-gradient source area, *Water Resour. Res.*, *31*, 1–10, 1995.

O'Loughlin, E. M., Saturation regions in catchments and their relation to soil and topographic properties, *J. Hydrol.*, *53*, 229–246, 1981.

Pearce, J. K., Forest engineering handbook: A guide for logging planning and forest road engineering, U.S. Bur. of Land Manage., Portland, Oreg., 1961.

Perkins, R. M., Climatic and physiographic controls on peakflow generation in the western Cascades, Oregon, Ph.D. dissertation, 190 pp., Oreg. State Univ., Corvallis, 1997.

Ramsay, F., and D. Schaefer, *The Statistical Sleuth.: A Course in Methods of Data Analysis*, Wadsworth, Belmont, Calif., 1997.

Reid, L. M., Sediment production from gravel-surfaced forest roads, Clearwater Basin, Washington, M.S. thesis, 247 pp., Univ. of Wash., Seattle, 1981.

Reid, L. M., and T. Dunne, Sediment production from road surfaces, *Water Resour. Res.*, *20*, 1753–1761, 1984.

Rothacher, J., C. T. Dyrness, and R. L. Fredriksen, Hydrologic and related characteristics of three small watersheds in the Oregon Cascades, Pac. Northwest For. and Range Exp. Stn., U.S. For. Serv., Corvallis, Oreg., 1967.

Snyder, K. U., Debris flows and flood disturbance in small, mountain watersheds, M.S. thesis, 53 pp., Oreg. State Univ., Corvallis, 2000.

Swanson, F. J., and C. T. Dyrness, Impact of clear-cutting and road construction on soil erosion by landslides in the Western Cascade, Oregon, *Geology*, *3*, 393–396, 1975.

Swanson, F. J., and M. E. James, Geology and geomorphology of the H. J. Andrews Experimental Forest, western Cascades, Oregon, *Res. Pap. PNW-188*, Pac. Northwest For. and Range Exp. Stn., U. S. For. Serv., Corvallis, Oreg., 1975.

Swanson, F. J., S. L. Johnson, S. V. Gregory, and S. A. Acker, Flood disturbance in a forested mountain landscape, *Bioscience*, *48*(9), 681–689, 1998.

Tague, C., and L. Band, Simulating the impact of road construction and forest harvesting on hydrologic response, *Earth Surf. Processes Landforms*, *26*, 135–151, 2001.

Thomas, R. B., and W. F. Megahan, Peak flow responses to clearcutting and roads in small and large basins, western Cascades, Oregon: A second opinion, *Water Resour. Res.*, *34*, 3393–3403, 1998.

Thomas, R. B., and W. F. Megahan, Reply to comment by J. A. Jones and G. E. Grant on "Peak flow responses to clear-cutting and roads in small and large basins, western Cascades, Oregon: A second opinion," *Water Resour. Res.*, *37*, 181–183, 2001.

Tsuboyama, Y., R. C. Sidle, S. Noguchi, and I. Hosoda, Flow and solute transport through the soil matrix and macropores of a hillslope segment, *Water Resour. Res.*, *30*, 879–890, 1994.

Wemple, B. C., Investigations of runoff production and sedimentation on forest roads, Ph.D. dissertation, 168 pp., Oreg. State Univ., Corvallis, 1998.

Wemple, B. C., J. A. Jones, and G. E. Grant, Channel network extension by logging roads in two basins, Western Cascades, Oregon, *Water Resour. Bull.*, *32*, 1195–1207, 1996.

Wemple, B. C., F. J. Swanson, and J. A. Jones, Forest roads and geomorphic process interactions, Cascade Range, Oregon, *Earth Surf. Processes Landforms*, *26*, 191–204, 2001.

Wigmosta, M. S., and W. A. Perkins, Simulating the effects of forest roads on watershed hydrology, in *Land Use and Watersheds: Human Influence on Hydrology and Geomorphology in Urban and Forest Areas*, *Water Sci. Appl. Ser.*, vol. 2, edited by M. Wigmosta and S. Burgess, pp. 127–143, AGU, Washington, D. C., 2001.

Woods, R., and L. Rowe, The changing spatial variability of subsurface flow across a hillside, *J. Hydrol. N. Z.*, *35*, 51–86, 1996.

Ziegler, A. D., and T. W. Giambelluca, Importance of rural roads as source areas for runoff in mountainous areas of northern Thailand, *J. Hydrol.*, *196*, 204–229, 1997.

Ziemer, R. R., and J. S. Albright, Subsurface pipeflow dynamics of north-coastal California swale systems, in *Erosion and Sedimentation in the Pacific Rim*, *IAHS Publ.*, *165*, 71–80, 1987.

J. A. Jones, Department of Geosciences, Oregon State University, Corvallis, OR 97331, USA.

B. C. Wemple, Department of Geography, University of Vermont, Burlington, VT 05405, USA. (bwemple@zoo.uvm.edu)